

(p , $2p$) Reactions at 600 MeV on Deuterium and Helium-4

C. F. PERDRISAT AND L. W. SWENSON*

College of William and Mary, Williamsburg, Virginia

AND

P. C. GUGELOT

University of Virginia, Charlottesville, Virginia

AND

E. T. BOSCHITZ, W. K. ROBERTS, AND J. S. VINCENT

Lewis Research Center, National Aeronautics and Space Administration, Cleveland, Ohio

AND

J. R. PRIEST

Miami University, Oxford, Ohio

(Received 5 March 1969)

The differential cross section ($d\sigma/dE d\Omega^2$) for (p , $2p$) reactions induced by 600-MeV protons on deuterium and helium-4 has been studied for symmetric reaction kinematics. By varying the detection angles of the two outgoing protons, we investigated the $D(p, 2p)n$ reaction for recoil momenta of the residual nucleus between 180 MeV/ c antiparallel and 370 MeV/ c parallel to the incident proton direction, respectively. For the $He^4(p, 2p)H^3$ reaction, the corresponding numbers are 148 and 298 MeV/ c , respectively. Some data for asymmetric reactions in helium-4 are also presented. Analyzing the data in terms of the plane-wave-impulse approximation, we calculate the single-proton momentum distribution in both nuclei. For deuterium, we observe a sudden change of slope in the momentum distribution around 150 MeV/ c , which cannot be explained with theoretical momentum distributions obtained by Fourier transforming Hulthén or Hamada-Johnston deuteron wave functions. In helium-4, the momentum distribution is nearly Gaussian up to about 180 MeV/ c ; above this value, an excess of large momentum components is observed. Both the deuterium and helium-4 results seem to indicate that the plane-wave impulse approximation is not valid at this energy and for the reaction parameters investigated here. Multiple scattering effects might be at the origin of the apparent excess of large Fermi momentum components obtained when the data are analyzed with the impulse approximation.

INTRODUCTION

PROTON quasi-elastic [or (p , $2p$)] reactions on nuclei have been investigated extensively in recent years over a range of energies up to 1000 MeV. These investigations have given a wealth of information pertaining to the separation energies, level widths, and momentum distribution¹ of proton hole states. Generally, a distorted-wave impulse approximation is used for the analysis of the data. The interaction of the incident and outgoing protons with the target nucleus is taken into account using either the optical-model² or a partial-wave analysis.³

Recent investigations of proton elastic scattering on nuclei at 1000 MeV⁴ and 600 MeV⁵ can be inter-

preted as evidence for the occurrence of multiple scattering with the individual nucleons. The analysis of these data requires a knowledge of the nuclear wave function or, equivalently, the Fermi momentum distribution. Although multiple scattering effects at these energies also distort the apparent momentum distribution calculated from a measurement of the (p , $2p$) differential cross section, the availability of data pertaining to both the elastic and quasi-elastic channels for a given nucleus will allow for a unified theoretical treatment of both reactions.

Here we report the experimental results of a measurement of the cross section for symmetric (p , $2p$) reactions on deuterium and helium-4 at 600 MeV, as well as some data for nonsymmetric (p , $2p$) events in helium-4. Emphasis was given to the extension of the measurement to as large a Fermi momentum q as possible: 370 MeV/ c in deuterium and 300 MeV/ c in helium-4.

The $D(p, 2p)$ reaction has been studied previously by Tyrén *et al.*⁶ at 460 MeV. However, the angular range covered was 35°–47°, corresponding to Fermi momenta smaller than 95 MeV/ c . A large hydrogen contamination in the target made the data unreliable in the range $|q| \leq 25$ MeV/ c . Data for $D(p, 2p)$ at 1000 MeV have been presented by the Brookhaven

* Present address: Department of Physics, Oregon State University Corvallis, Ore.

¹ M. Riou, *Rev. Mod. Phys.* **37**, 375 (1965).

² G. Jacob and T. A. J. Maris, *Rev. Mod. Phys.* **38**, 121 (1966); T. Berggren and H. Tyrén, *Ann. Rev. Nucl. Sci.* **16**, 153 (1966).

³ D. F. Jackson and T. Berggren, *Nucl. Phys.* **62**, 353 (1965).

⁴ Deuterium: G. W. Bennett, J. L. Friedes, H. Palevsky, R. J. Sutter, G. J. Igo, W. D. Simpson, G. C. Phillips, R. L. Stearns, and D. M. Corley, *Phys. Rev. Letters* **19**, 387 (1967); helium-4: H. Palevsky, J. L. Friedes, R. J. Sutter, G. W. Bennett, G. J. Igo, W. D. Simpson, G. C. Phillips, D. M. Corley, N. S. Wall, R. J. Stearns, and B. Gottschalk, *Phys. Rev. Letters* **18**, 1200 (1967).

⁵ Deuterium: J. S. Vincent, E. T. Boschitz, W. K. Roberts, K. Gotow, P. C. Gugelot, C. F. Perdrisat, and L. W. Swenson, *Bull. Am. Phys. Soc.* **13**, 872 (1968); helium-4: E. T. Boschitz, W. K. Roberts, J. S. Vincent, K. Gotow, P. C. Gugelot, C. F. Perdrisat, and L. W. Swenson, *Phys. Rev. Letters* **20**, 1116 (1968).

⁶ H. Tyrén, S. Kullander, O. Sundberg, R. Ramachandran, P. Isacson, and T. Berggren, *Nucl. Phys.* **79**, 321 (1966).

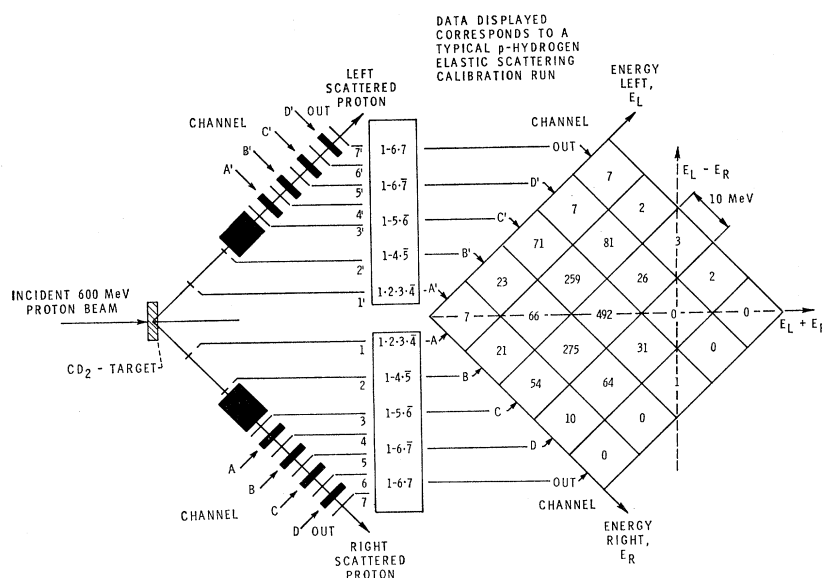


FIG. 1. Schematics of the apparatus used in this experiment. The numbers in the 5 by 5 matrix are typical for a p -H calibration run at 41° .

Cosmotron collaboration (Simpson *et al.*⁷). In the limited region of Fermi momentum available for comparison (the 1000-MeV data do not extend beyond 100-MeV/ c Fermi momentum), these results are compatible with the ones presented here. In an earlier investigation, Leksin⁸ had measured the differential p - p cross section for quasi-elastic scattering at 660 MeV and scattering angles of 50° – 90° in the c.m. system of the colliding protons. Leksin concluded that the differential cross section differed only slightly when the target proton is free or bound in deuterium.

The $\text{He}^4(p, 2p)$ reaction has also been studied by Tyrén *et al.*⁶ These data extend from 150 to 175 MeV/ c Fermi momentum parallel and antiparallel to the incident proton, respectively.

In the present work, the results for both deuterium and helium-4 are analyzed in terms of the plane-wave impulse approximation (PWIA). Within the PWIA, the laboratory differential cross section ($d\sigma/dE d\Omega_1 d\Omega_2$) for $(p, 2p)$ is directly related to the free p - p c.m. differential cross section ($d\sigma/d\Omega$)_{pp} (Berggren and Jacob⁹) by

$$\begin{aligned} & (d\sigma/dE d\Omega_1 d\Omega_2) \\ &= (\text{kinematic factor}) (d\sigma/d\Omega)_{pp} [N_l \rho(q)/(l+1)], \quad (1) \end{aligned}$$

where $\rho(q)$ is the probability density for a proton with Fermi momentum $\mathbf{q} = -\mathbf{q}_R$, and \mathbf{q}_R is the recoil momentum of the residual nucleus. N_l is the number of protons in a state of the target nucleus with orbital

angular momentum l . The momentum probability of the target proton is $\rho(q) = |\phi(q)|^2$, where $\phi(q)$ is the single-proton wave function in momentum space. The kinematic factor when the two outgoing protons have equal energies and angles to the beam (symmetric geometry) is given by

$$(\text{kinematic factor}) = 4 \frac{p^2 m_p^2 c^4 + p^2 c^2 \sin^2 \theta}{p_0 (m_p^2 c^4 + q^2 c^2)^{1/2}}. \quad (1')$$

The momenta of the two outgoing protons were calculated from the measured laboratory angles θ and energies E . The “missing” momentum obtained from the known incident momentum \mathbf{p}_0 is identified with the recoil momentum \mathbf{q}_R of the residual nucleus:

$$\mathbf{q}_R = \mathbf{p}_0 - (\mathbf{p}_1 + \mathbf{p}_2), \quad (2)$$

where \mathbf{p}_0 , \mathbf{p}_1 , and \mathbf{p}_2 are the incident and two outgoing laboratory proton momenta, respectively. In this experiment, we selected reactions with equal angles and energies for the two protons in the exit channel. As a result, only events with nuclear recoil \mathbf{q}_R either parallel or antiparallel to the incident proton direction were detected; this situation corresponds to 90° scattering angles in the center of mass of the two-proton system. Furthermore, the recoil momentum is zero for symmetric kinematics and for laboratory angles given by

$$\cos \theta_0^{\text{lab}} = p_0/2p.$$

Here $p = |\mathbf{p}_1| = |\mathbf{p}_2|$ is the outgoing momentum of either proton; p is obtained from energy conservation

$$(p^2 c^2 + m_p^2 c^4)^{1/2} = \frac{1}{2}(E_0 - E_s) + m_p c^2, \quad (3)$$

where E_0 is the incident proton energy; E_s is the separation energy of the target proton. For deuterium $E_s = 2.2$ MeV, whereas for He^4 it is 20.4 MeV. Angles

⁷ W. D. Simpson, H. Palevsky, J. L. Friedes, G. W. Bennett, R. J. Sutter, B. Gottschalk, G. J. Igo, D. M. Corley, N. S. Wall, and R. L. Stearns, *Bull. Am. Phys. Soc.* **13**, 632 (1968); and report, 1969 (unpublished).

⁸ G. A. Leksin, *Soviet Phys.—JETP* **5**, 371 (1957).

⁹ T. Berggren and G. Jacob, *Nucl. Phys.* **47**, 481 (1963).

TABLE I. Deuterium data.

θ_{lab} [deg]	q_R [MeV/c]	$d_R/dE d\Omega^2$ [mb/MeV sr ²]	E_{pp}^{lab} [MeV]	$(d\sigma/d\Omega)_{pp}^{90^\circ\text{c.m.}}$ [mb/sr]	$\rho(q_R)$ [10 ³ (MeV/c) ³ sr] ⁻¹
28	181	0.047±0.020	384	3.70	0.0059±0.0025
30	160	0.044±0.022	405	3.60	0.0055±0.0028
32	137	0.047±0.019	429	3.50	0.0058±0.0024
34	110	0.165±0.035	457	3.40	0.0207±0.0043
36	85	0.69±0.10	488	3.25	0.087±0.0125
	82	0.52±0.09	488	3.25	0.065±0.0110
37	70	0.57±0.08	506	3.20	0.0714±0.0102
	67.5	0.73±0.11	506	3.20	0.0915±0.0133
38	55.5	1.43±0.15	524	3.10	0.184±0.020
	52	1.70±0.17	524	3.10	0.218±0.022
39	41	2.88±0.20	544	3.02	0.375±0.026
	36	3.15±0.22	544	3.02	0.41±0.028
40	28.5	4.34±0.25	565	2.95	0.57±0.033
	20	5.66±0.29	565	2.95	0.75±0.038
41	22.5	6.10±0.32	588	2.85	0.82±0.044
	10	8.4±0.41 ^a	588	2.85	1.15±0.056
42	21.5	5.41±0.30	612	2.65	0.78±0.043
	29.5	3.84±0.24	612	2.65	0.55±0.034
43	40	2.26±0.18	638	2.35	0.365±0.028
	44.5	2.19±0.17	638	2.35	0.354±0.027
44	59.5	1.17±0.13	666	2.10	0.21±0.024
	63	0.91±0.11	666	2.10	0.163±0.019
45	83	0.31±0.016	696	1.87	0.0623±0.0034
	85.5	0.34±0.06	696	1.87	0.0686±0.0012
46	102.5	0.16±0.018	727	1.75	0.034±0.0039
	104.5	0.25±0.057	727	1.75	0.0529±0.0122
48	149	0.047±0.007	797	1.40	0.0126±0.0018
50	200	0.013±0.0056	877	1.15	0.0043±0.0019
52	254.5	0.0086±0.0018	968	0.92	0.0037±0.0008
54	313.5	0.0053±0.0009	1071	0.74	0.0029±0.00046
56	370	0.0030±0.0009	1176	0.60	0.0022±0.00067

^a The cross section for this point is obtained after a 38% correction due to the target hydrogen content. The error does not include the uncertainty in the hydrogen content.

which agrees with range curves obtained for the two protons in p - p scattering. The range telescope efficiencies had been determined previously.⁵

The best resolution for the recoil momentum components along the beam, transverse in and transverse out of the scattering plane, was 16.4, 16.2, and 11.4 MeV/c, respectively (FWHM). The corresponding values for the largest recoil momentum investigated (370 MeV/c) were 43.5, 19.4, and 35.1. The longitudinal momentum uncertainty is largely determined by the angular resolution in the reaction plane, whereas the uncertainty on the transverse component in the reaction plane is dependent primarily upon the energy resolution. The uncertainty on the transverse out component is determined by the vertical angular acceptance.

A coincidence background was observed and had to

be subtracted from the data. The main source of background was due to quasi-elastic reactions on the carbon in the CD₂ target. The carbon background was determined by measuring the coincidence rate using a matched graphite target. Because the carbon background was measured exactly in the same way as the angular distribution from the CD₂ target, all sources of systematic errors cancel out except the ratio of the number of C nuclei in the CD₂ and graphite targets and the difference in target energy losses. The difference in energy losses for the CD₂ and graphite targets was corrected in the analysis. The background originates predominantly from (p , $2p$) reactions on the $p_{3/2}$ state in carbon, which reaches a peak at a recoil momentum of about 100 MeV/c and goes through a minimum at the zero-recoil angle. We observed a maximum in the background around 37°

and 45° . At these angles the background accounted for about 20% of the raw data. The relative background correction increases for angles larger than 45° and smaller than 37° . At 56° the carbon background was 45% of the raw data. At 45° we found for the $C^{12}(p, 2p)$ reaction leading to the ground state of B^{11} a differential cross section $(d\sigma/dE d\Omega^2) = 180 \pm 12 \mu\text{b}/\text{MeV sr}^2$. This result can be compared with the numbers quoted by Tyrén *et al.*⁸ at 460 MeV/c, obtained by range technics and with a magnetic spectrometer: $200 \pm 25 \mu\text{b}/\text{MeV sr}^2$ and $165 \pm 30 \mu\text{b}/\text{MeV sr}^2$, respectively.

The data were also corrected for accidental coincidences. The accidental rate was measured by delaying the coincidence signature of one of the telescope relative to the other by about 56 nsec, which corresponds to the time microstructure of the beam. Although the beam was extracted from the synchrocyclotron "stochastically," the chance coincidence corrections were found to increase sharply for the smallest angles investigated. It was 50% of the data at 28° but negligible for angles larger than 34° . The flux of protons with good time structure was typically $4\text{--}7 \times 10^8/\text{sec}$. The electronic logic was gated off during the prompt part of each burst (about 2 msec at 18-msec intervals). The accidental counting rate could not be measured simultaneously with data taking, and hence contains uncertainties larger than the statistical error. The largest uncertainty is due to the instability in the structure of the stretched beam. The systematic error on the subtracted rates could be as large as 50% at 28° , but is completely negligible above 34° .

The data presented were obtained by adding the events with a summed proton energy within ± 20 MeV from the energy value corresponding to the absorption maximum. Two methods were used: (1) the position of the maximum was chosen from the expected range, and (2) the position of the maximum was chosen from a least-square fitting procedure with position of the maximum a free parameter. The results obtained in these two ways are compatible within statistical uncertainty. We observed that the carbon background accounted for the spectrum outside of the 4-channel region defined above.

The cross section $(d\sigma/dE d\Omega^2)$ calculated for each angle is presented as a function of angle in Table I and Fig. 3. In Table I, q_R is calculated as the square root of the quadratic sum of the longitudinal momentum and weighted-average transverse momentum obtained from the kinematical parameters, p_0 , p and θ in the initial and final states. In the angular region where the transverse component of the recoil momentum is not small compared to the longitudinal component ($36^\circ\text{--}45^\circ$), the cross sections for transverse momentum within ± 10 MeV/c and within 10–30 MeV/c are given separately. Outside this angular region we included all events within the energy range defined above (transverse momentum within ± 30

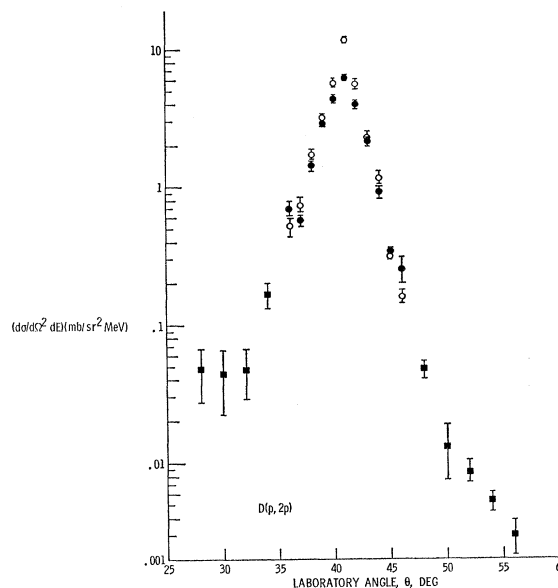


FIG. 3. Differential cross section for $D(p, 2p)$ with equal angles and energies left and right. The data points with different transverse recoil momenta are indicated by \circ for $-10 < q_{\perp} < +10$, \bullet for $10 < |q_{\perp}| < 30$ MeV/c, and \square for $|q_{\perp}| < 30$ MeV/c, respectively.

MeV/c). Events with transverse recoil momentum on either side of the beam were considered equivalent.

The absolute cross section was obtained by using a monitoring telescope downstream from the CD_2 target. The monitoring telescope was calibrated by $C^{12}(p, pn)$ activation measurement.¹²

The momentum distribution $\rho(q)$, where q is now the Fermi momentum obtained from Eq. (2) with $\mathbf{q} = -\mathbf{q}_R$, was calculated from Eq. (1). In this experiment the Fermi momentum resulted in equivalent laboratory collision energies in the two-proton system varying between 384 and 1176 MeV (Fermi momenta from -181 MeV/c to $+370$ MeV/c, parallel to the incoming proton and antiparallel, respectively). For the range of equivalent laboratory collision energies involved, the factor $(d\sigma/d\Omega)_{pp}$ in formula (1) varies considerably. We used the values given in Table I, which were obtained from the data available below 660-MeV lab energy¹³ and above 2200 MeV.¹⁴ At 1000 MeV, $(d\sigma/d\Omega)_{pp}$ has been measured by Dowell *et al.*,¹⁵

¹² We used the value $\sigma = 30.2 \pm 1.8$ mb, obtained by I. D. Prokoshkin and A. A. Tiapkin, Soviet Phys.—JETP **5**, 148 (1957).

¹³ M. H. MacGregor, R. A. Arndt, and R. M. Wright, University of California Radiation Laboratory Report No. 50426, 1967 (unpublished).

¹⁴ A. R. Clyde, University of California Radiation Laboratory Report No. 16275, 1966 (unpublished); C. W. Akerlof, R. H. Hieber, A. D. Krish, K. W. Edwards, L. G. Ratner, and K. Ruddick, Phys. Rev. **159**, 1138 (1967).

¹⁵ J. D. Dowell, W. R. Frisken, G. Martelli, B. Musgrave, M. B. van der Raay, and R. Rubinstein, Nuovo Cimento **18**, 818 (1960).

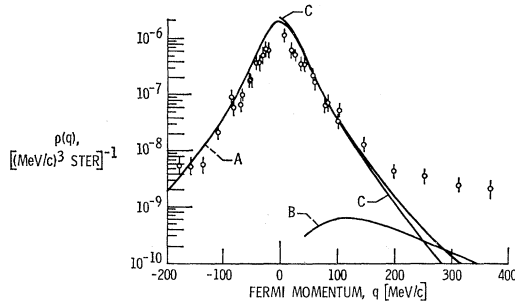


FIG. 4. Momentum distribution for the proton in deuterium obtained with the plane-wave impulse approximation. The Fermi momentum is taken as minus the residual nucleus recoil momentum. The part of the momentum scale to the right of the origin is for recoil along the incident proton direction. Curve A is the square of the Fourier transform of the S -state Hulthén wave function. Curve B is for a pure D -state proton normalized to 0.07 and corresponds to a Hulthén D -state wave function of the form given in Ref. 19. Curve C is for the S -state Hamada-Johnston wave function.

Bugg *et al.*,¹⁶ and McFarlane *et al.*¹⁷ The results from these three sources are not quite compatible with each other. We have assumed McFarlane's value and obtained the cross section values at intermediate energies by visual interpolation.

Figure 4 presents the Fermi momentum distribution for the proton in the deuteron, as obtained from formula (1) (see also Table I). The Fermi distribution is not corrected for finite resolution. A detailed correction is difficult because the data are analyzed in terms of a resulting momentum

$$|\mathbf{q}| = (q_{\parallel}^2 + q_{\perp}^2 + q_{out}^2)^{1/2}$$

and the elementary volume element in Fermi momentum space is not a cube in the Cartesian coordinate system $(q_{\parallel}, q_{\perp}, q_{out})$ where q_{\parallel} , q_{\perp} , and q_{out} are the components parallel, transverse in, and transverse out of the scattering plane, respectively. To discuss the quality of the data, we can, however, define an average momentum resolution width (FWHM)

$$\langle \Delta q \rangle_{av} = (\Delta q_{\parallel} \times \Delta q_{\perp} \times \Delta q_{out})^{1/3}. \quad (4)$$

For $q \sim 0$, $\langle \Delta q \rangle_{av}$ is 14.5 MeV/c and for $q \sim 300$ MeV/c it is 31 MeV/c. An estimate of the correction for finite resolution assuming a Gaussian momentum resolution curve of width equal to $\langle \Delta q \rangle_{av}$ gives +15% at $q \sim 0$. The correction vanishes around $q = 50$ MeV/c and is smaller than -5% above 50 MeV/c. The error in the absolute cross section due to uncertainties in the efficiency and solid angles of the telescopes and

the $C^{12}(p, pn)C^{11}$ cross section is estimated to be less than $\pm 25\%$.

One may notice in Fig. 4 that, up to a Fermi momentum of about 150 MeV/c, $\rho(q)$ is in approximate agreement with a momentum distribution obtained by Fourier-transforming a Hulthén¹⁸ S -state deuteron wave function:

$$\psi^S(\text{Hulthén})(r) = (c/r) [\exp(-\alpha r) - \exp(-\beta r)],$$

where

$$c = [1/(2\pi)^{1/2}] [\alpha\beta(\alpha+\beta)]^{1/2}/(\beta-\alpha)$$

is the normalization constant. Curve A in Fig. 4 corresponds to a S -state Hulthén wave function with $\alpha = 0.232 \text{ fm}^{-1}$ and $\beta = 1.202 \text{ fm}^{-1}$ ($c = 0.269 \text{ fm}^{-1/2}$), values which were found best for a 2-parameter fit to the pion exchange potential solution of Gartenhaus¹⁹ (see Moravcsik²⁰). Above 150 MeV/c, there is a definite discrepancy between our data and the Hulthén S -state momentum distribution. Curve B in Fig. 4 is a D -state momentum distribution obtained by Fourier-transforming the Hulthén D -state wave function as given in Ref. 19, and furthermore assuming the deuteron to consist of a pure D -state, again using Eq. (1). The D -state normalization is taken to be 0.07. Although it is evident that at large Fermi momenta the D -state contributes an important part of the momentum distribution, it will not account for all of the discrepancy. We have also investigated the momentum distributions to be expected from S - and D -state wave functions obtained by Hamada and Johnston²¹ from a nucleon-nucleon potential model which reproduces the two-nucleon data below 315 MeV. The hard-core radial functions can be well approximated by a linear combination of exponential terms:

$$\psi_{HJ}^S(r) = r^{-1} \sum_{i=1}^n a_i \exp(-b_i r).$$

With $n=4$, the fit to the Hamada-Johnston functions u and w is better than 3% in the radius range 0.57 to 11.3 fm. The S -state momentum distributions vanishes at a momentum corresponding to the radius of the hard-core (400 MeV/c). The rapid decrease of the S -state distribution can be seen in Fig. 4, curve C. A similar result was obtained with a wave function from a one-boson-exchange potential.²²

We conclude that our momentum distribution cannot be explained from known deuteron wave functions *within* the plane-wave impulse approximation. The deviation between our data and the prediction of the PWIA with Hulthén S -wave momentum distribution is best seen in Fig. 5, which is a plot of the ratio of the Fermi momentum densities $\rho(q)$ from our data

¹⁶ D. V. Bugg, A. J. Oxley, J. A. Zoll, J. G. Rushbrooke, V. E. Barnes, J. B. Kinson, W. P. Dodd, G. A. Doran, and L. Riddiford, *Phys. Rev.* **133**, B1017 (1964).

¹⁷ W. K. McFarlane, R. J. Homer, A. W. O'dell, E. J. Sacharidis, and G. H. Eaton, University of Birmingham Report No. 13, 1962 (unpublished).

¹⁸ L. Hulthén, *Arkiv. Mat. Astron. Fysik* **28A**, No. 5 (1942).

¹⁹ S. Gartenhaus, *Phys. Rev.* **100**, 900 (1955).

²⁰ M. J. Moravcsik, *Nucl. Phys.* **7**, 113 (1958).

²¹ T. Hamada and I. D. Johnston, *Nucl. Phys.* **34**, 382 (1962).

²² K. Bleuler, K. Erkelenz, and K. Holinde, report of work prior to publication, 1968; and (private communication).

and $\rho(\text{Hulthén})(q)$ obtained from formula (1). It is seen in Fig. 5 that the ratio $\rho(q)/\rho(\text{Hulthén})(q)$ is approximately a constant within the range $-50 \leq q \leq +50 \text{ MeV}/c$, but that outside this region it increases strongly. We note that the large discrepancy observed at Fermi momenta larger than $150 \text{ MeV}/c$ corresponds to distances smaller than 1.3 fm . The deuteron wave functions discussed above may not be valid at such small distances.

We might add that the differential cross section for breakup of the deuteron has been evaluated by Bertocchi,²³ using the multiple scattering theory proposed by Glauber.²⁴ Although the calculations of Bertocchi are relevant to reaction kinematics very different from ours, one might infer from his discussion that double scattering will result in a sudden decrease of the slope of the differential cross section, with possibly an interference effect similar to that observed in elastic p - D scattering. The expected dip in the breakup cross section would appear at a momentum transfer depending upon the reaction kinematics.

HELIUM-4 RESULTS

The helium-4 experiment²⁵ utilized a liquid target. The target volume was defined by the intersection of the solid angles of the two telescopes (counters 1-2 and 1'-2' in Fig. 2). For all angles investigated, more than 99% of the beam intercepted the target volume

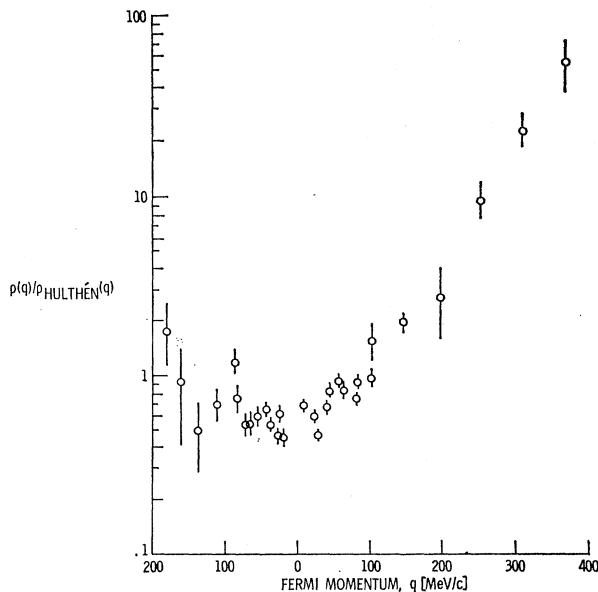


FIG. 5. Ratio of the PWIA momentum distributions for the data and for a S -state Hulthén wave function $\rho(q)/\rho(\text{Hulthén})(q)$.

²³ L. Bertocchi, *Nuovo Cimento* **50A**, 1015 (1967).

²⁴ R. T. Glauber, in *Lectures in Theoretical Physics*, edited by Wesley E. Brittin *et al.* (Wiley-Interscience Publishers, Inc., New York, 1959), Vol. I.

²⁵ C. F. Perdriat, P. C. Gugelot, L. W. Swenson, E. T. Boschitz, and W. K. Roberts, *Bull. Am. Phys. Soc.* **13**, 568 (1968).

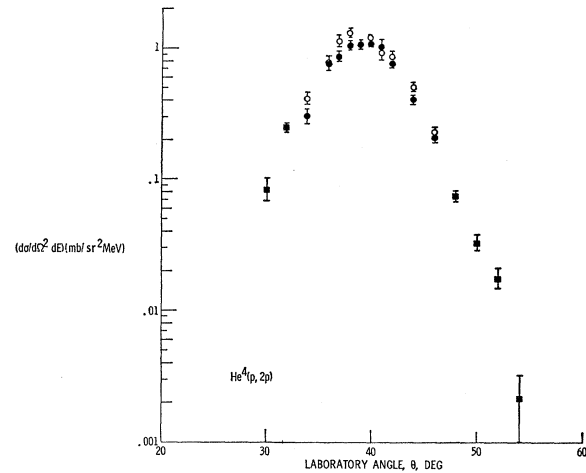


FIG. 6. Differential cross-section for $\text{He}^4(p, 2p)$ with equal angles and energies left and right. The data points with different transverse recoil momenta are indicated by \circ for $-10 < q_{\perp} < +10$, \bullet for $10 < |q_{\perp}| < 30 \text{ MeV}/c$, and \square for $|q_{\perp}| < 30 \text{ MeV}/c$, respectively.

as defined. The effective target thickness for 40° scattering angles was 4.0 cm , to be compared with the diameter of the cylindrical target vessel, which was 10 cm . Here, as for the deuterium experiment, the geometry was changed during data taking in such a way as to get optimum resolution for recoil momenta close to zero and to increase the counting rate at the largest momenta. The ratio of maximum to minimum solid angles for each telescope was ~ 2.7 , with a corresponding ratio of effective target lengths of ~ 1.2 . The combined effects of the geometry changes gave an increase in counting rate of a factor 9. The energy resolution was 16 MeV . A run taken with empty target produced no measurable background for the angular range covered (30° – 54°). However, as for deuterium, the accidental coincidence rate increased sharply at the smallest angles investigated. The accidental coincidence correction was at the most 25% at 30° . The results were treated in the same way as explained for deuterium, considering between 34° and 46° the data with transverse momentum smaller than $10 \text{ MeV}/c$ and between 10 and $30 \text{ MeV}/c$ separately, but adding all events with transverse momenta up to $30 \text{ MeV}/c$ outside of this angular region. The cross section was calculated assuming the density of liquid helium to be 0.124 g cm^{-3} and using the calculated solid angle.

The cross section is presented in Table II and Fig. 6, together with the corresponding recoil momenta calculated relativistically. The momentum distribution $\rho(q)$ for one proton in helium-4 is shown in Fig. 7 (see also Table II). To obtain $\rho(q)$ we have used the values for the free p - p cross section $(d\sigma/d\Omega)_{pp}$ indicated in Table II.

A Gaussian radial wave function would give a Gaussian momentum distribution which, in Fig. 7,

TABLE II. Helium-4 data.

θ_{lab} [deg]	q_R [MeV/c]	$d\sigma/dE d\Omega^2$ [mb/MeV sr ²]	E_{pp}^{lab} [MeV]	$(d\sigma/d\Omega)_{pp}^{90^\circ\text{c.m.}}$ [mb/sr]	$\rho(q_R)$ [$10^6(\text{MeV}/c)^3 \text{sr}^{-1}$]
30	148.4	0.083±0.013	417	3.55	0.0053±0.0009
32	122.4	0.248±0.016	444	3.42	0.0162±0.0011
34	95.8	0.311±0.044	477	3.30	0.0205±0.0030
	93	0.419±0.057	477	3.30	0.0275±0.0038
36	67.1	0.768±0.083	512	3.18	0.051±0.0055
	63.1	0.787±0.096	512	3.18	0.053±0.0065
37	52.7	0.876±0.089	529	3.11	0.059±0.0055
	47.5	1.13±0.12	529	3.11	0.076±0.008
38	39.1	1.05±0.044	547	3.03	0.072±0.003
	31.7	1.31±0.063	547	3.03	0.089±0.0045
39	28.3	1.07±0.038	571	2.92	0.075±0.0025
	16.6	1.08±0.051	571	2.92	0.076±0.0038
40	25.3	1.20±0.051	592	2.75	0.089±0.004
	10.8	1.10±0.044	592	2.75	0.082±0.0035
41	24.1	1.02±0.11	613	2.55	0.080±0.0085
	33.2	0.92±0.10	613	2.55	0.073±0.008
42	41.5	0.876±0.07	638	2.30	0.076±0.006
	47.4	0.774±0.057	638	2.30	0.067±0.005
44	79	0.508±0.041	692	1.95	0.051±0.004
	82.8	0.406±0.032	692	1.95	0.041±0.003
46	118.9	0.229±0.035	752	1.60	0.028±0.0045
	121.1	0.209±0.019	752	1.60	0.0255±0.0025
48	161.7	0.075±0.0076	814	1.35	0.011±0.0011
50	205.4	0.033±0.0051	884	1.12	0.0056±0.00085
52	250.9	0.0178±0.0032	960	0.94	0.0037±0.00065
54	298.2	0.0021±0.0011	1042	0.80	0.0005±0.00027

would be represented by a parabola. Curve A in Fig. 7 is a least- χ^2 fit for a Gaussian through the data points with Fermi momentum within ± 120 MeV/c. In the high-momentum region the distribution is not in good agreement with a Gaussian wave function. A definitive deviation occurs at about 180 MeV/c. The excess of high-momentum components observed in helium-4 and that seen in deuterium might have common origin, although the deviation is definitively more striking in deuterium than in helium-4.

There is also a definite asymmetry between the values of $\rho(q)$ for Fermi momentum antiparallel and parallel to the incident proton momentum, the former kinematical situation giving systematically larger values of $\rho(q)$ than the latter. A least- χ^2 fit indicates that the most likely shift is 4 MeV/c and that the χ^2 value does not change when the position of the maximum is taken as a free parameter. We obtain $\chi^2=60$ in both cases, with 20 and 19 degrees of freedom, respectively. Such asymmetries are expected on the basis of calculations in distorted-wave impulse approximation, as shown for example by Berggren and Jacob⁹ for scattering on *S*-state protons in O^{16} at 460 MeV.

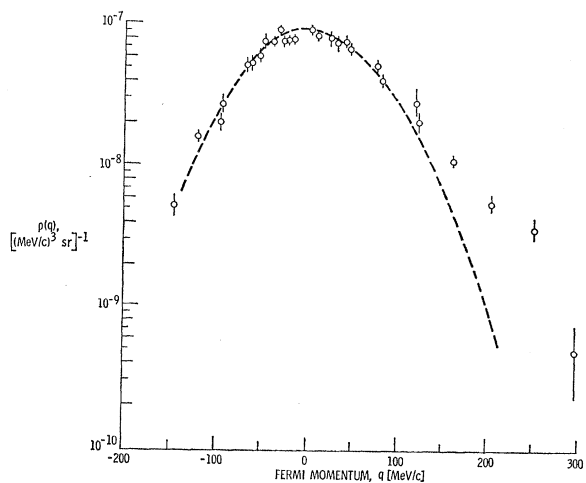


FIG. 7. Momentum distribution for one proton in He^4 obtained with the PWIA. Curve A is a least- χ^2 fit with a Gaussian through the data with $|q| \leq 120$ MeV/c.

The smallness of the shift observed in the maximum of the momentum distribution might allow a naive picture for the interaction with the nucleus: The incident proton scatters elastically with the nucleus before the $(p, 2p)$ event occurs and gives to the nucleus a small momentum $\Delta\mathbf{q}_R$ along the beam direction. Hence we measure a recoil momentum:

$$\mathbf{q}_{R'} = \mathbf{q}_R + \Delta\mathbf{q}_R.$$

As we identify the Fermi momentum with $-\mathbf{q}_{R'}$ instead of the unobservable \mathbf{q}_R , the maximum of the observed momentum distribution will occur at $\mathbf{q}_{R'} = +\Delta\mathbf{q}_R$, i.e., for a residual Fermi momentum antiparallel to the beam direction and equal to $|\Delta\mathbf{q}_R|$, in agreement with the data. Following a quasi-elastic $(p, 2p)$ event, the two outgoing protons move perpendicular to the beam direction in their c.m. system by the very choice of symmetric reaction kinematics made here. The resulting transverse momentum given to the nucleus from elastic scattering in the exit channel vanishes on the average in the scattering plane. We expect, however, a widening of the transverse momentum distribution, which should be best seen by measuring $(p, 2p)$ kinematics with nonzero transverse Fermi momentum. We would expect the shift along the beam direction to be $p_0(1 - \cos\bar{\theta}) \cong \frac{1}{2}p_0^2$ and the increase in width transversally to the beam to be $p_0 \sin\bar{\theta}$, where $\bar{\theta}$ is the average scattering angle in elastic p -He⁴ scattering.

We have measured asymmetric reactions with Fermi momentum component transverse to the beam up to 145 MeV/ c , and zero longitudinal component.²⁶ A least- χ^2 fit through the asymmetric data gives a half-width at $1/e$ of 110 MeV/ c , instead of 90 MeV/ c for the longitudinal distribution. The increase in width observed corresponds to an additional transverse momentum of about 64 MeV/ c . The average elastic scattering angle $\bar{\theta}$ we obtain from the longitudinal shift of the momentum distribution is 0.066 ± 0.015 rad, whereas the average angle from the widening of the transverse momentum distribution is 0.053 ± 0.020 rad. If we calculate the average elastic-scattering angle

from the p -He⁴ elastic scattering data at 600 MeV (Ref. 5), we obtain 0.096 rad.

We note that the He⁴ $(p, 2p)$ data by Tyrén *et al.*⁶ at 460 MeV correspond to a differential cross section at $q=0$ of 0.69 ± 0.07 mb/MeV sr² to be compared with our result 1.2 ± 0.1 mb/MeV sr². The size of the error bars in the tails of the distribution at 460 MeV does not allow a conclusion about a deviation from the impulse approximation. Neither is a shift of a few MeV/ c in the position of the maximum incompatible with these data.

CONCLUSION

We have observed a definite discrepancy in the internal momentum distribution calculated from the D $(p, 2p)$ data assuming the PWIA as compared with the distribution for several typical deuteron wave functions. This result may indicate that the PWIA is not valid at 600 MeV and that the interaction of the incoming proton with the neutron in deuterium plays an important role. It will be necessary to perform a double scattering calculation to see whether the multiple scattering theory for nucleon-nucleus reactions does explain the deviation from the PWIA. Such data together with the elastic p -D data at the same energy may ultimately provide the best deuteron wave function for use in other calculations.

The momentum distribution obtained from the He⁴ $(p, 2p)$ data indicates also a possible disagreement with the PWIA if one assumes a Gaussian radial wave function—although here the discrepancy is less evident. A slight shift in the position of the helium-4 momentum distribution maximum is shown to be compatible with an elastic scattering process in the input channel. However, since the energy resolution was about 16 MeV, the possibility for unbound final states makes any conclusion about the validity of the PWIA uncertain in the case of helium-4.

ACKNOWLEDGMENTS

We would like to thank the staff of the Space Radiation Effects Laboratory for their support. Our thanks also to the Brookhaven National Laboratory and to R. Gibbs for the loan of the liquid-helium target. We wish further to acknowledge many valuable discussions with Dr. E. Remler.

²⁶ Data for asymmetric kinematics in C¹² $(p, 2p)$ at 160 MeV have been obtained previously by B. Gottschalk, K. H. Wang, and K. Strauch [Nucl. Phys. A90, 83 (1967)].